Synthetic Access to L-Guluronic Acid via Fluorine-Directed C-5 Epimerization

Nicholas W. See, Norbert Wimmer, Guoqing Zhang, Elizabeth H. Krenske and Vito Ferro*

School of Chemistry and Molecular Biosciences, The University of Queensland, Brisbane QLD 4072, Australia

ABSTRACT

L-Guluronic acid is integral to the structures of alginates and to the pathogenesis of *Pseudomonas aeruginosa*. The exploitation of this hexose in both existing and new contexts is, however, limited by its prohibitively high commercial cost. We report on a short and efficient synthetic route to an L-GulA building block from a simple D-mannose thioglycoside. In this synthesis, the fluorine-directing effect is exploited to achieve a stereoselective C-5 epimerization. DFT calculations illuminate the substituent effects which operate to confer this selectivity.

INTRODUCTION

Alginates **1** constitute a class of marine polysaccharides of exceptional importance to the food, materials, and pharmaceutical industries.[1] These glycans are also key to the pathogenesis of *Pseudomonas aeruginosa* pulmonary infections in cystic fibrosis patients.[2] Perhaps of equal significance is their structural complexity (Figure 1). The alginate framework is a heterogeneous assembly of D-mannuronic acid (D-ManA) and L-guluronic acid (L-GulA) monomeric units. Across the entire scaffold, 1,4-glycosidic linkages unite these subunits into alternating and block polymeric sequences of varied length. With this considered, further to the 1,2-*cis* configuration of the individual glycosidic bonds and the highly charged nature of the alginate scaffold, an appreciation for the difficulties inherent to the construction of these natural products is obtained.

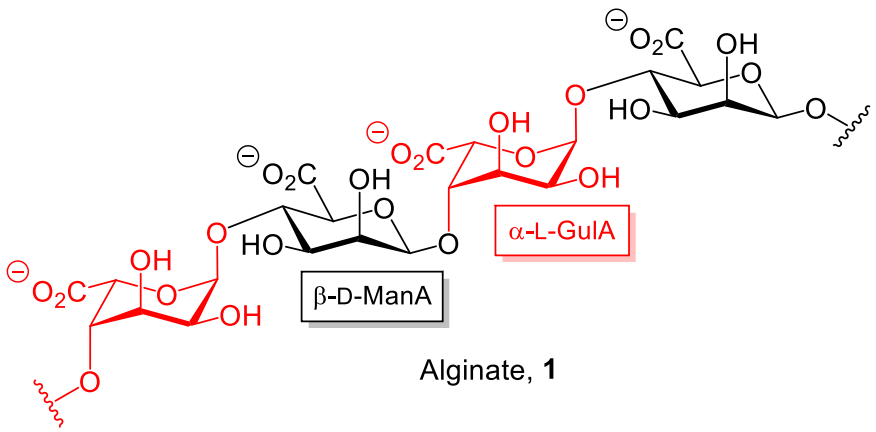

Alginate, **1**

Figure 1. A representative alternating copolymer sequence of alginate **1**.

An early contribution to this field was made by the van der Marel research group who demonstrated the solution-phase synthesis of an alginate D-ManA trisaccharide.[3] In subsequent studies with Codée, the construction of the analogous oligomer containing L-GulA[4] and a mixed sequence fragment[5] were both achieved. Excellent reviews of alginate synthesis are provided by Clausen,[6] Cai[7] and Codée;[8] all precede the very recent advance of Yang[9] who has

since reported the synthesis of the longest poly-D-ManA fragment achieved to-date. Notably, access to gram-scale quantities of alginate building blocks is only reasonable through chemical synthesis. This is the direct consequence of the prohibitively high costings of both D-ManA and L-GulA whose sodium salts, at present, are priced at $21,030/g and $30,750/g, respectively.[10] While D-ManA is typically accessed via the oxidation of D-mannose,[11] the application of this protocol to L-GulA is less appealing as the requisite starting material, L-gulose, is reasonably expensive ($600/10 g).[10] Its synthesis from cheaper L-gulonic acid γ-lactone has been demonstrated but is somewhat lengthy (12 steps).[4]

With an ongoing research interest in the synthesis of rare L-hexoses,[12] we sought an alternative route to L-GulA to expedite progress in the fields of alginate and glycosaminoglycan mimetic[13] synthesis. We reasoned that a fluorine-directing effect, which has so far been explored for the synthesis of L-iduronic acid[12a] and L-idose[12b] derivatives, could be exploited for this purpose. Fluorine-directed syntheses of L-hexoses feature the free radical reductions of 5-*C*-bromo sugars, the stereoselectivity of which is considerably improved by a β-fluoride. In the presence of a different anomeric substituent, the appropriate D-hexose typically forms as the major product. This is particularly pertinent to 5-*C*-bromo sugars of D-mannose for which an α-fluoride confers complete D-hexose reduction stereoselectivity.[14] A β-fluoride, however, generates a preparative amount of the desired L-gulose product. For the synthesis of L-iduronic acid (L-IdoA), we have shown that a combination of a β-fluoride, acetate protecting groups (PG) and a C-6 methoxycarbonyl provides optimal reduction stereoselectivity.[12a] We now report on the synthesis of 5-*C*-bromide **2** which bears these substituents and show that its free radical reduction is indeed stereoselective for L-GulA derivative **3** (Scheme 1).

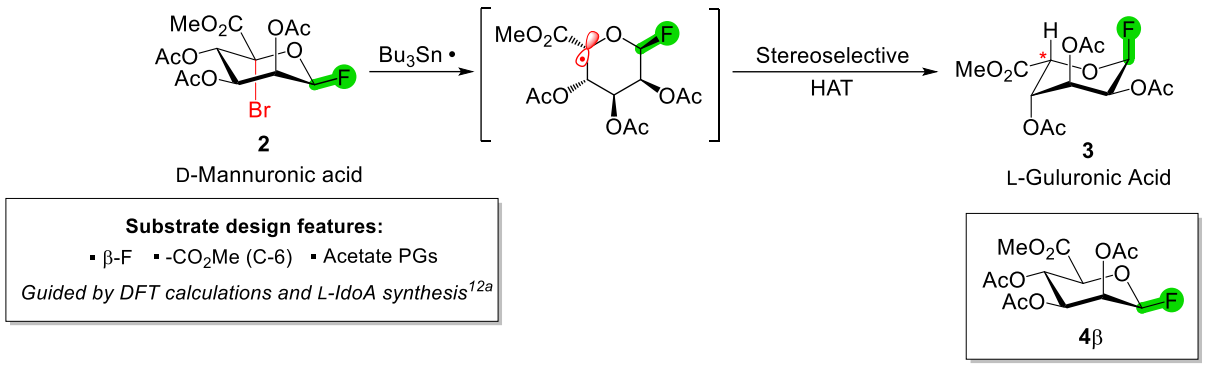

Scheme 1. The fluorine-directed synthesis of L-GulA derivative **3** features the free radical reduction of 5-*C*-bromide **2**.

RESULTS AND DISCUSSION

Prediction of Reduction Stereoselectivity

Prior to commencing the synthesis of **2**, we elected to predict the stereoselectivity of its free radical reduction. Density functional theory (DFT) was used to calculate transition states (TSs) for the selectivity-determining step of this reaction, namely the hydrogen atom transfer (HAT) to the *C*-5 radical intermediate. Given its success in our previous studies of these reactions,[12] we employed the same computational approach to our present work. TS geometries were optimized with B3LYP/6-31G(d)-LANL2DZ after which single point energy calculations were performed at the B3LYP-D3(BJ)/def2-TZVPP level of theory. Solution-phase Gibbs free energies were subsequently calculated. The solvent (toluene) was modelled implicitly using the Solvation Model based on Solute Electron Density (SMD) method[15] and for simplicity, *n*-Bu_3SnH was modelled with Me_3SnH.

Five major TSs were located on the potential energy surface for this reaction. The structures of these TSs are shown in Figure 2 with their associated enthalpies and Gibbs free energies. **TS1** and **TS2** lead to L-GulA product **3** and feature $^1C_4$ chair and ^2S_O skew-boat

conformations, respectively. The remaining three structures – **TS3**, **TS4** and **TS5** – deliver D-ManA derivative **4**β. Respectively, the pyranose rings of these TSs take up $^4C_1$ chair, $^1C_4$ chair and ^2S_O boat conformations. Within each set, the TSs differ only by the conformation of the pyranose ring. It therefore dictates their relative energies.

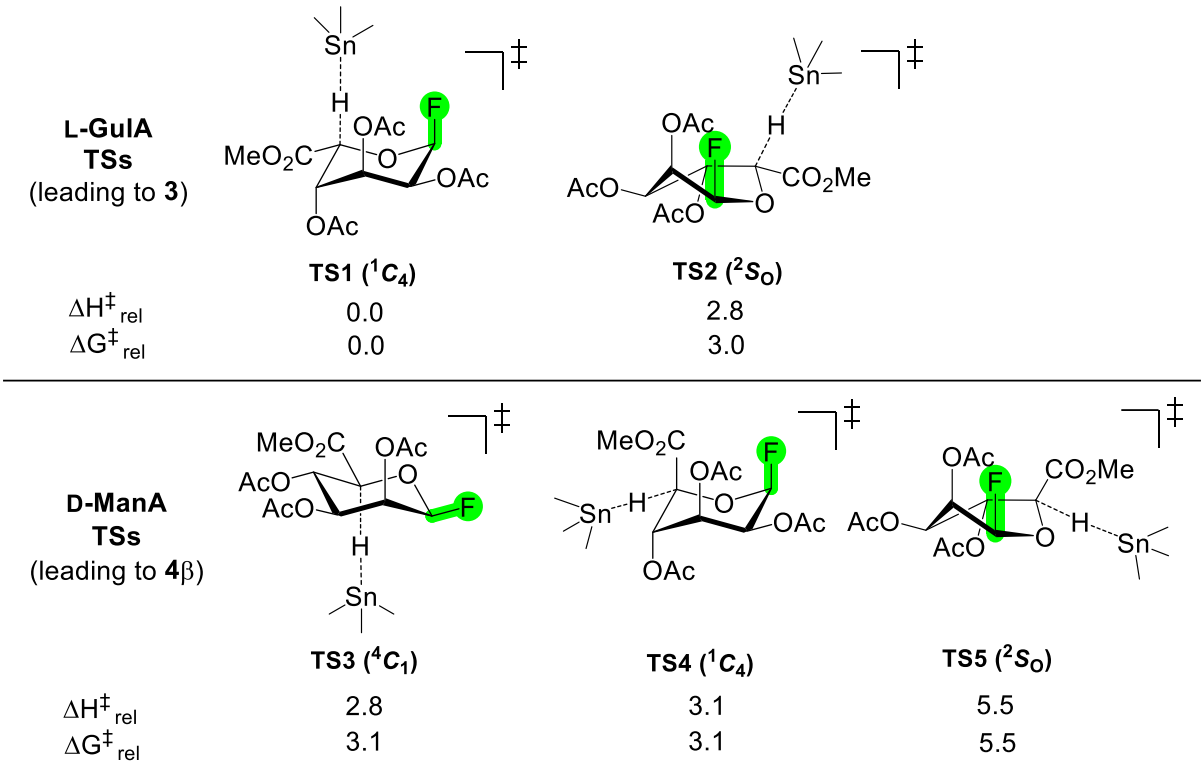

Figure 2. Computed TSs for the free radical reduction of 5-*C*-bromide **2**. Structures were calculated at the B3LYP-D3(BJ)/def2-TZVPP-SMD(PhMe)//B3LYP/6-31G(d)-LANL2DZ-SMD(PhMe) level of theory. Energies are reported in units of kcal/mol.

The results indicate that **TS1** is the major contributor; the remaining TSs are all at least 3.0 kcal/mol higher in energy and therefore do not contribute significantly to the reaction. Based on a Boltzmann analysis of all TSs, a theoretical stereoselectivity of 99:1 at 25 ºC was calculated for the reduction of **2** in favour of the desired L-GulA derivative **3**.

To understand the high stereoselectivity predicted for this reaction, we analysed the structure of **TS1** and compared it to those of **TS3** and **TS4** which are equienergetic and the lowest energy TSs leading to D-ManA product **4β**. Their structures are shown in Figure 3. A series of stabilising hyperconjugative interactions is operative in these TSs. These effects involve key interactions between σ-donors and σ-acceptors. To maximise orbital overlap and therefore stabilisation, an anti-arrangement of a σ-donor and acceptor is essential. The forming C-H bond at C-5 can be regarded as a surrogate for an unpaired electron and is capable of adopting either role.[16] In both **TS1** and **TS3**, the radical is stabilised by an *anti* endocyclic oxygen lone pair (LP_O). This $LP_O \longrightarrow \sigma^*_{C5\text{-}H}$ interaction is absent in **TS4** in which the groups are arranged in a *gauche* fashion.

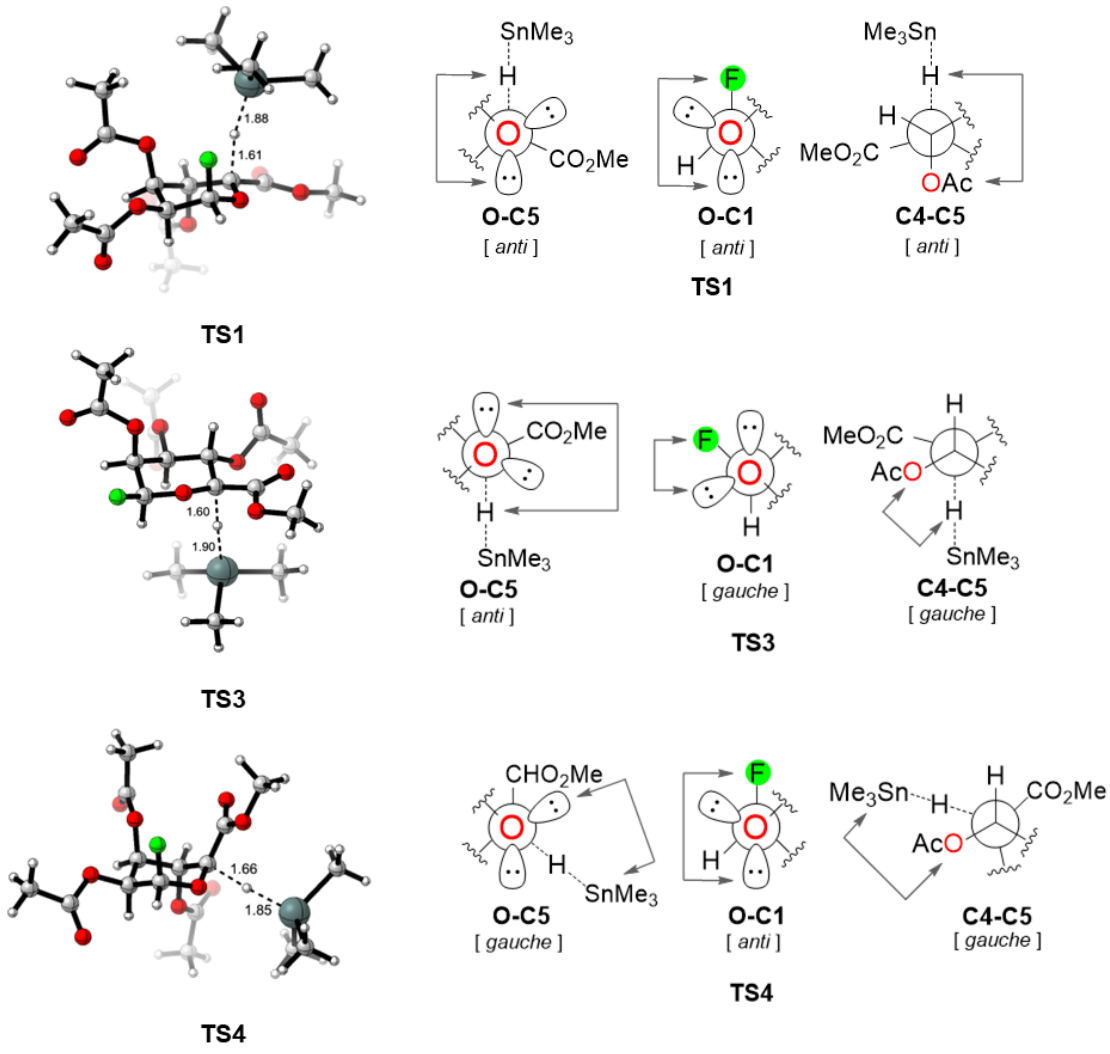

Figure 3. Optimised geometries of **TS1**, **TS3** and **TS4**. For each TS, Newman projections of three selected bonds are displayed adjacently. The key arrangements of stabilising groups (LP_O, β-F, C-4 OAc) about each of these bonds are listed underneath.

We next examined the role of the β-fluoride. Consistent with our existing understanding of the fluorine-directing effect, a LP_O is *anti* to the C-F bond in **TS1**. In less stable **TS3**, these groups take up a *gauche* arrangement from which weaker stabilisation is derived. In this way, the *endo*-anomeric effect is engaged in **TS1** but not **TS3** to drive L-GulA stereoselectivity. A $LP_O \longrightarrow \sigma^*_{C\text{-}F}$ interaction is also operative in **TS4**. However, it would appear that the TS

stability derived from this interaction is offset by the unfavourable equatorial approach of the stannane to the C-5 radical.

Further analysis of the TSs showed that the OAc group at C-4 likely plays a role in stabilising theses TSs. In **TS1**, the forming C-H bond overlaps effectively with the $\sigma^*_{C4\text{-}O}$ orbital. With poorer overlap of these orbitals, less stabilisation is provided by the C-4 ester in both **TS3** and **TS4**. It is therefore apparent that through a synergy of stereoelectronic effects, the β-F and C-4 OAc groups both underpin the high stereoselectivity predicted for the reduction of **2**.

Validation Through Chemical Synthesis

Encouraged by the theoretical prediction, we embarked on the synthesis of 5-*C*-bromide **2** (Scheme 2). We commenced its preparation with the regioselective *O*-tritylation of commercially available thioglycoside **5**. Following complete consumption of **5**, acetic anhydride was introduced to the same pot to convert the hydroxyl groups of triol **6** to *O*-acetyl esters. Consequently, orthogonally protected thioglycoside **7** was produced in high yield (74%) after purification on silica. The 6-OH group of **7** was then liberated in good yield (80%) through the action of $BF_3{\cdot}OEt_2$ in dilute CH_2Cl_2 and with methanol as a cation scavenger. The resulting alcohol **8** was then oxidized according to the procedure of van der Marel.[11] Accordingly, treatment of **8** with catalytic (2,2,6,6-tetramethylpiperidin-1-yl)oxyl (TEMPO) and stoichiometric $PhI(OAc)_2$ facilitated swift conversion to the corresponding carboxylic acid with no evidence of concurrent *S*-oxidation. Following aqueous workup and azeotropic drying with toluene, the crude product was dissolved in dry *N*,*N*-dimethylformamide (DMF) and alkylated under basic conditions with iodomethane. Subsequent chromatographic purification provided methyl ester **9** in high yield (80%).

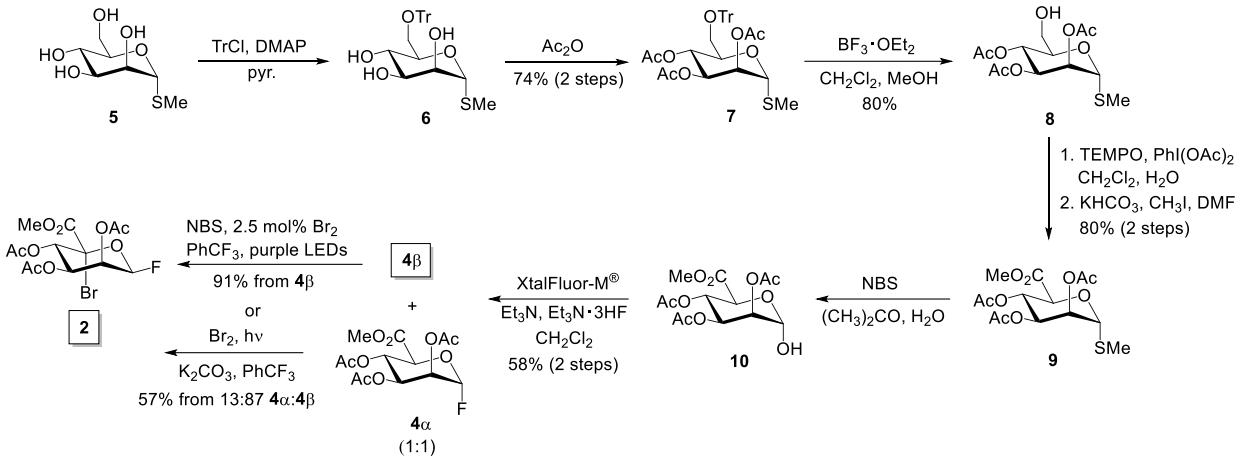

Scheme 2. The preparation of 5-*C*-bromide **2** was undertaken from thioglycoside **5**.

We next directed our attention towards introducing the anomeric fluoride. The direct conversion of thioglycosides to glycosyl fluorides is typically achieved by the method of Nicolaou which employs hazardous *N*,*N*-diethylaminosulfurtrifluoride (DAST) and which generally delivers anomeric mixtures.[17] Within our laboratory, we have recently improved the safety of this conversion by developing a protocol which uses a combination of *N*-bromosuccinimide (NBS), XtalFluor-M® and $Et_3N{\cdot}3HF$.[18] This method is particularly effective for the synthesis of β-D-glycosyl fluorides. However, per-*O*-acylated D-mannose thioglycosides are fluorinated with high α-stereoselectivity. Thus, reasoning that **9** would likely succumb to the same fate, we explored alternative fluorination methods.

Fortuitously, deoxyfluorination (XtalFluor-M®/$Et_3N{\cdot}2HF$) of hemiacetal **10**, which was readily obtained via the NBS-mediated hydrolysis of **9**, delivered equimolar amounts of α- and β-D-mannosyl fluorides **4α** and **4β**. To achieve this quantity of **4β**, initiation at low temperature and close reaction monitoring were both imperative, as was the use of $Et_3N{\cdot}2HF$ which offers a superior source of nucleophilic fluoride to $Et_3N{\cdot}3HF$.[19] Spectroscopically, **4α** and **4β** were distinguished by their $^2J_{C\text{-}F}$ coupling constants (**4α**: 38.2 Hz, **4β**: 20.9 Hz).[14]

Nuclear Overhauser effect (NOE) correlations between the anomeric proton and both H-3 and H-5 in **4β** were also observed. Unfortunately, **4α** and **4β** were largely inseparable on silica gel.[20] Analytical samples of each anomer were however obtained by crystallizing chromatographically enriched fractions from EtOAc/*n*-hexane. The X-ray crystal structures of **4α** and **4β** are shown in Figure 4.[21]

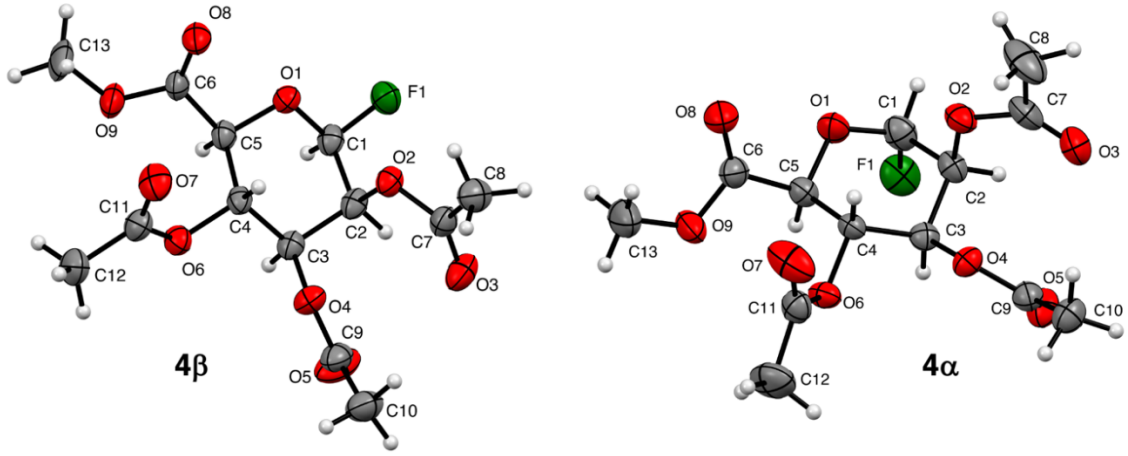

Figure 4. ORTEP plots of D-mannosyl fluorides **4β** and **4α** (shown with 50% ellipsoid probability).

With a view to harnessing the Ferrier photo-bromination[22] to complete the synthesis of **2**, we postulated that compared to **4β**, α-D-mannosyl fluoride **4α** would demonstrate poorer reactivity towards these conditions.[14] This can be understood by examining the rate-determining step of the Ferrier photo-bromination which features the reversible bromine-mediated abstraction of a hydrogen atom from C-5 (Figure 5a).[22b] The associated forward and reverse processes are respectively characterised by rate constants k_1 and k_{-1}. We considered that the electron-withdrawing effect of the axially disposed fluoride would slow C-H bond homolysis in **4α** (i.e., k_1 (**4β**) >> k_1 (**4α**)). The endocyclic oxygen (LP_O), which plays an

essential role in stabilising the forming C-5 radical, is delocalised into the C-F bond. In this way, its ability to aid radical generation is limited (Figure 5b). A secondary factor which also ought to retard the photolysis of **4α** is a destabilising 1,3-diaxial interaction between the α-fluoride and the S_H2 process taking place at C-5. With the fluoride disposed in an equatorial position in **4β**, these effects can be considered negligible.

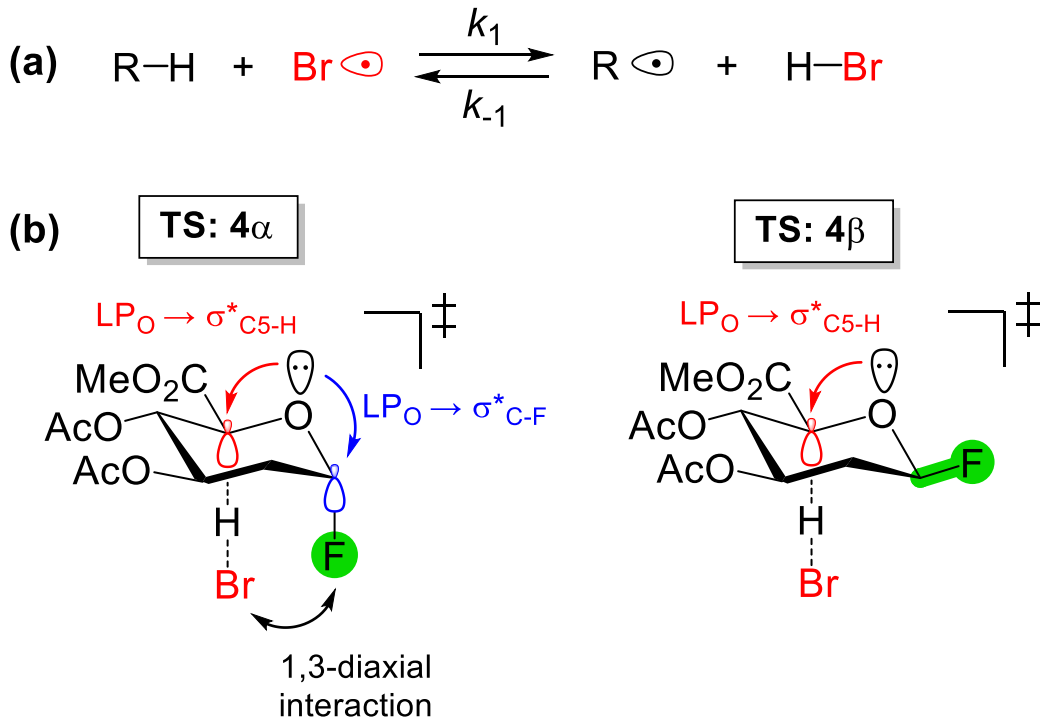

Figure 5. D-Mannosyl fluorides **4α** and **4β** are predicted to display different reactivities towards Ferrier photo-bromination. (a) Kinetic scheme for the rate-determining step of the reaction and (b) structural differences between TSs for C-H bond homolysis in **4α** and **4β**.

Photolysis of a dilute, chromatographically-enriched 13:87 mixture of **4α** and **4β** with Br_2 in anhydrous $PhCF_3$ gratifyingly provided an anomerically pure sample of β-configured 5-*C*-bromide **2** in moderate yield (57%). Indeed, **4α** had failed to react under the prescribed

conditions thus enabling a "photochemical resolution" of the β-anomer from the mixture.[23] Bromination at C-5 was indicated by the disappearance of the H-5 proton, the resolution of H-4 to a doublet spin system and a substantial downfield shift of the C-5 signal (**4β**: 72.0 ppm, **2**: 88.9 ppm). HRMS data were also consistent with the structure of **2**. We have recently developed an improved protocol for the carbon tetrachloride-free Ferrier photo-bromination under mild conditions (≤40 °C) that can be performed on a gram scale (manuscript in preparation). The reaction employs a compact photoreactor equipped with purple LEDs (λ = 405 nm) which provide a more controlled light source and less heat compared with a typical 500 W tungsten lamp. A solution of pure **4β**, obtained via recrystallization of the 13:87 α/β mixture, was thus subjected to our optimized protocol (0.16 M in $PhCF_3$, 3 eq. NBS, 2.5 mol% Br_2, 405 nm, 6 h) to give **2** in excellent yield (91%).

Free radical reduction of **2** generated a mixture of C-5 epimers of which the desired L-GulA derivative **3** was the major component (Scheme 3). Specifically, treatment of **2** with *n*-Bu_3SnH and Et_3B in anhydrous toluene at room temperature generated L-GulA derivative **3** and **4β** in a ratio of 82:18 and in very high yield (93%). Upon inverting the configuration at C-5, an expected shift in the preferred conformation of the pyranose ring from a $^4C_1$ to a $^1C_4$ chair was indicated by the small $^3J_{H\text{-}H}$ values measured for **3**. We also observed that the *trans* diaxial arrangement of the fluorine and H-2 nuclei within **3** yielded a large heteronuclear coupling constant (26.0 Hz). Pleasingly, the experimental stereoselectivity was in agreement with the theoretical prediction. This highlighted the success of the computational approach employed.

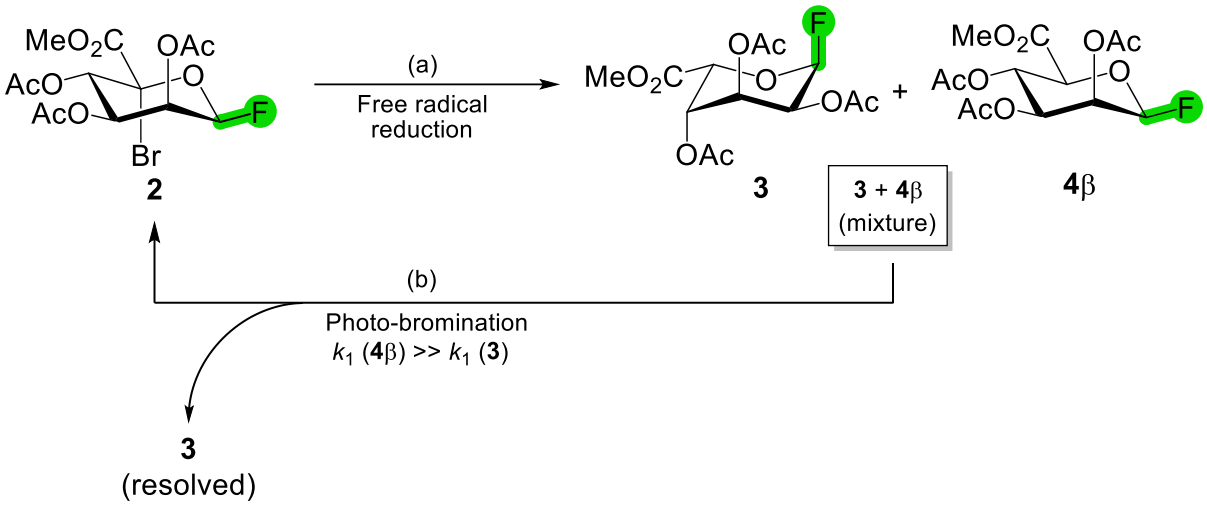

Scheme 3. Free radical reduction of **2** yields an inseparable mixture of **3** and **4β**. Photochemical resolution of this mixture delivers separable **3** and 5-*C*-bromide **2**. (a) *n*-Bu_3SnH, Et_3B, O_2, PhMe, r.t., 50 min (**3**:**4β**: 82:18; yield: 93%); $InCl_3$, Et_3SiH, Et_3B, O_2, CH_3CN, 0°C → r.t., 20 min (**3**:**4β**: 87:13; yield: 83%); (b) Br_2, hν, K_2CO_3, $PhCF_3$, 70°C, 1h, **3**: 42%, **4β**: 21%.

Having now established a short and efficient route to L-GulA derivative **3**, we aimed to improve the practicality of our method in two ways. Firstly, we acknowledged its dependence on stoichiometric *n*-Bu_3SnH. This reagent is toxic and iterative chromatography was required to separate the associated organotin byproducts from the mixture of **3** and **4β**. During our explorations of less hazardous reduction protocols, including catalysis in *n*-Bu_3SnH,[24] a reverse polarity catalysis approach[25] and $(Me_3Si)_3SiH$,[26] all of which had been optimized by others on simple alkyl halides, we quickly discovered significant incompatibilities with carbohydrate scaffolds.[27] However, exposure to $InCl_2H$, generated *in situ* from $InCl_3$ and Et_3SiH,[28] rapidly effected the free radical reduction of **3**. The reaction was high yielding (83%) and proceeded

with higher stereoselectivity (87:13) than the *n*-Bu_3SnH reduction. This is possibly accounted for by solvent effects and/or the smaller steric bulk of the hydrogen atom donor.

Secondly, we aimed to address the lack of separability of **3** from its C-5 epimer, **4β**. Inspired by the successful photochemical resolution of **2** from the mixture of **4β** and **4α** and noting that the anomeric configuration of **3** (α, axial) opposes that of **4β** (β, equatorial), we considered that the same chemistry could be applied to this problem. With k_1 (**4β**) >> k_1 (**3**) underpinned by a set of structural features analogous to those shown in Figure 5b, we proposed that **4β** would photo-brominate at a higher rate than **3** to enable separation. Confirming this hypothesis, a controlled photo-bromination of an 82:18 mixture of **3** and **4β** generated pure samples of largely unreacted **3** (42% isolated yield) and **2** (21% isolated yield) – the latter of which is self-evidently recyclable through subsequent reduction.

CONCLUSIONS

We have established a simple and efficient fluorine-directed synthesis of L-GulA derivative **3** from commercially available D-mannose thioglycoside **5**. DFT calculations correctly predicted the stereoselectivity of the free radical reduction of **2** and therefore guided the construction of **3**. The calculations principally indicated that the substrate design features used for the previously undertaken fluorine-directed synthesis of L-IdoA were applicable to this study.[12a] Conveniently, compound **3** is endowed with glycosyl donor capability[29] and is conceivably amenable to protecting group substitutions. In accordance with our previous studies,[14] we have also shown that α- and β-configured mannosyl fluorides demonstrate different reactivities towards Ferrier photo-bromination. This enabled the isolation of both **2** and **3** from their appropriate stereoisomeric mixtures via a photochemical resolution.

Furthermore, we have improved practicality of the fluorine-directing effect methodology by replacing CCl_4 with $PhCF_3$ and irradiating with purple LEDs in the Ferrier photobromination, and replacing *n*-Bu_3SnH with $InCl_3$/Et_3SiH for the hydrogen atom transfer. This work will importantly expedite progress in both new and existing research programs which require access to preparative amounts of L-GulA.

EXPERIMENTAL SECTION

General

Reagents were purchased from Merck and Co. and were used without further purification. All reactions were performed in oven-dried glassware and were monitored by thin layer chromatography (TLC) using silica gel F_{254} aluminium-backed sheets. Except where indicated, photo-brominations were performed with an Arlec 500 W tungsten lamp fitted with a linear halogen tube. The lamp was strictly held at a 20 cm distance from the reaction vessel. Compounds were visualised using *p*-anisaldehyde/H_2SO_4 dip. NMR spectra were measured on Bruker Avance 300 and 500 MHz spectrometers and referenced to the residual solvent peaks (δ_H = 7.26 ppm, δ_C = 77.0 ppm). ^{19}F NMR spectra were externally referenced to monofluorobenzene (δ_F = -113.5 ppm). 2D NMR experiments including ^1H-^1H COSY, ^1H-^{19}F COSY and HSQC aided with structure elucidations and signal assignments. Optical rotations were measured on a Jasco P-2000 polarimeter. Melting points were measured on a Digimelt MPA161 apparatus. Low- and high-resolution electrospray ionisation mass spectrometry (LRMS/HRMS) data were obtained with Bruker HCT and Bruker micrOTOF$_Q$ spectrometers, respectively, in positive ionisation mode. Flash chromatography was performed on silica gel (230-400 mesh, Grace) under pressure with specified eluants. Reaction stereoselectivities were measured by ^1H NMR analysis of the post-workup product mixture, prior to purification by flash chromatography.

Synthesis

Methyl 2,3,4-tri-*O*-acetyl-1-thio-6-*O*-triphenylmethyl-α-D-mannopyranoside (7): To a solution of methyl 1-thio-α-D-mannopyranoside **5** (1.1 g, 5.1 mmol) and DMAP (2 mg) in anhydrous pyridine (20 mL) was added triphenylmethyl chloride (1.8 g, 6.6 mmol) in one portion. The solution was stirred under $N_{2(g)}$ for 4 h at 50 °C after which it was cooled in an ice-bath (external Dewar temperature: 4 °C) and treated with acetic anhydride (1.7 mL, 18.4 mmol) – added dropwise over 10 min. The reaction was then allowed to attain r.t. before it was stirred for a further 48 h. Excess acetic anhydride was destroyed with anhydrous methanol (13 mL) before the product was concentrated under reduced pressure. The resulting orange syrup was dissolved in EtOAc (100 mL) and washed with water (100 mL). The aqueous phase was extracted with EtOAc (2 × 75 mL). The combined organic phases (pH = 5) were then washed with sat. $NaHCO_3$ (2 × 75 mL); pH 7; and brine (75 mL). The product was dried ($MgSO_4$), filtered and concentrated to dryness. Residual pyridine was azeotropically removed with PhMe. Purification by flash chromatography (PhMe/EtOAc 20:1) gave the *trityl ether* **7** as a colourless oil (2.3 g, 74%). R_f = 0.18 (*n*-hexane/EtOAc 6:1; stains brown with *p*-anisaldehyde/H_2SO_4 dip). $[\alpha]_D$ +68.0 (*c.* 0.5, $CHCl_3$). ^{1}H NMR (500 MHz, $CDCl_3$): δ 7.46 – 7.44 (m, 6H, Ph), 7.31 – 7.28 (m, 6H, Ph), 7.25 – 7.22 (m, 3H, Ph), 5.34 – 5.33 (m, 1H, H-3), 5.27 – 5.25 (m, 2H, H-2, H-4), 5.21 (br s, 1H, H-1), 4.28 – 4.27 (m, 1H, H-5), 3.23 (dd, 1H, part A of ABX system, $J_{5,6a}$ = 5.6 Hz, $J_{6a,6b}$ = 10.5 Hz, H-6a), 3.19 (dd, 1H, part B of ABX system, $J_{5,6b}$ = 2.5 Hz, H-6b), 2.23 (s, 3H, -SCH_3), 2.18 (s, 3H, -CH_3), 1.97 (s, 3H, -CH_3), 1.75 (s, 3H, -CH_3). ^{13}C NMR (125 MHz, $CDCl_3$): δ 170.0, 169.9, 169.4 (3 × C=O), 143.7, 137.9, 129.0, 128.7, 128.2, 127.8, 127.0, 125.3 (Ph), 86.7 (-*C*Ph_3), 82.9 (C-1), 71.0 (C-3), 70.6 (C-5), 69.7 (C-4), 66.8 (C-2), 62.5 (C-6), 20.9, 20.7, 20.5 (3 × -CH_3), 13.4 (SCH_3). HRMS: calcd for $C_{32}H_{34}O_8SNa$ 601.1872 [M + Na]$^+$; found 601.1848 [M + Na]$^+$.

Methyl 2,3,4-tri-*O*-acetyl-1-thio-α-D-mannopyranoside (8): $BF_3{\cdot}OEt_2$ (5.0 mL, 41 mmol) was added dropwise over 10 min to a vigorously stirred solution of the trityl ether **7** (10.9 g, 34.2 mmol) and dry methanol (15 mL) in dry CH_2Cl_2 (900 mL) at r.t. under $Ar_{(g)}$. The reaction was stirred for a further 5 min after which the reaction mixture was washed with water (150 mL), sat. $NaHCO_3$ (150 mL) and brine (150 mL) before it was dried ($MgSO_4$), filtered and concentrated under a stream of $N_{2(g)}$. Purification by flash chromatography (PhMe/EtOAc 3:1) gave the *alcohol* **8** as a colourless syrup (9.2 g, 80%). R_f = 0.25 (PhMe/EtOAc 3:1; stains brown with *p*-anisaldehyde/H_2SO_4 dip). $[\alpha]_D$ +75.8 (*c.* 1.2, $CHCl_3$). ^{1}H NMR (500 MHz, $CDCl_3$): δ 5.37 (dd, 1H, $J_{1,2}$ = 1.6 Hz, $J_{2,3}$ = 3.2 Hz, H-2), 5.33 (dd, 1H, $J_{3,4}$ = 9.9 Hz, H-3), 5.27 (dd, 1H, $J_{4,5}$ = 10.0 Hz, H-4), 5.18 (d, 1H, H-1), 4.14 – 4.09 (m, 1H, H-5), 3.71 (ddd, 1H, part A of ABXY system, $J_{5,6a}$ = 2.5 Hz, $J_{6a,6b}$ = 12.8 Hz, $J_{6a,OH}$ = 8.5 Hz, H-6a), 3.65 (ddd, 1H, part B of ABXY system, $J_{5,6b}$ = 4.1 Hz, $J_{6b,OH}$ = 5.7 Hz, H-6b), 2.37 (dd, 1H, -OH), 2.15 (s, 3H, -CH_3), 2.14 (s, 3H, -CH_3), 2.08 (s, 3H, -CH_3), 1.99 (s, 3H, -CH_3).^{13}C NMR (125 MHz, $CDCl_3$): δ 170.9, 169.9, 169.8 (3 × C=O), 83.6 (C-1), 70.9 (C-5), 70.8 (C-2), 69.2 (C-3), 66.6 (C-4), 61.3 (C-6), 20.9, 20.7, 20.6 (3 × -CH_3), 13.8 (SCH_3). HRMS: calcd for $C_{13}H_{20}O_8SNa$ 359.0777 [M + Na]$^+$; found 359.0757 [M + Na]$^+$.

Methyl (methyl 2,3,4-tri-*O*-acetyl-1-thio-α-D-mannopyranosid)uronate (9): The alcohol **8** (9.1 g, 27 mmol) was vigorously stirred with (diacetoxyiodo)benzene (18 g, 54 mmol) and TEMPO (850 mg, 5.4 mmol) in a mixture of CH_2Cl_2 (300 mL) and water (90 mL) for 1.5 h. The reaction mixture was then diluted with EtOAc (200 mL) before it was washed with sat. $Na_2S_2O_3$ (50 mL) and brine (50 mL). The product was dried ($MgSO_4$), filtered and concentrated to dryness to give the crude carboxylic acid as an orange oil, which was then taken up in dry DMF (200 mL) and treated with finely powdered $KHCO_3$ (5.4 g, 54.4 mmol) and iodomethane

(2.5 mL, 41 mmol). The reaction was stirred o/n in the dark at r.t. under $Ar_{(g)}$ before it was concentrated under a stream of $N_{2(g)}$. The crude residue was dissolved in EtOAc (200 mL) and washed with water (50 mL). The aqueous phase was extracted with EtOAc (3 × 50 mL) after which the combined organic phases were washed with water (50 mL) and brine (50 mL). The product was dried ($MgSO_4$), filtered and concentrated to dryness to yield a brown syrup. Purification by flash chromatography (PhMe/EtOAc 7:1 → 5:1 → 4:1) furnished the *methyl ester* **9** as a light-yellow syrup (7.9 g, 80%, 2 steps). R_f = 0.24 (PhMe/EtOAc 7:1; stains brown with *p*-anisaldehyde/H_2SO_4 dip). $[\alpha]_D$ + 80.4 (*c.* 0.53, $CHCl_3$). ^{1}H NMR (500 MHz, $CDCl_3$) δ 5.42 (dd, 1H, $J_{3,4} = J_{4,5}$ = 8.4 Hz, H-4), 5.33 (dd, 1H, $J_{1,2} = J_{2,3}$ = 3.4 Hz, H-2), 5.30 (dd, 1H, H-3), 5.27 (d, 1H, H-1), 4.67 (d, 1H, H-5), 3.78 (s, 3H, CO_2CH_3), 2.20 (s, 3H, -CH_3), 2.13 (s, 3H, -CH_3), 2.08 (s, 3H, -CH_3), 2.01 (s, 3H, -CH_3). ^{13}C NMR (125 MHz, $CDCl_3$): δ 169.9, 169.7, 169.5, 168.1 (4 × C=O), 82.7 (C-1), 70.4 (C-5), 69.4 (C-2), 68.5 (C-3), 67.5 (C-4), 52.8 (CO_2CH_3), 20.9, 20.7, 20.6 (3 × -CH_3), 13.6 (SCH_3). HRMS: calcd for $C_{14}H_{20}O_9SNa$ 387.0726 $[M + Na]^+$; found 387.0708 $[M + Na]^+$.

Methyl (2,3,4-tri-*O*-acetyl-α-D-mannopyranose)uronate (10): To a stirred solution of the methyl ester **9** (7.9 g, 21.7 mmol) and water (6.5 mL) in acetone (130 mL) at 0 °C was added NBS (18 g, 102 mmol) portion-wise over a 5 min period. Stirring was continued for 45 min at the same temperature before it was cautiously quenched with a 1:1 mixture of 5% $Na_2S_2O_3$/sat. $NaHCO_3$ (100 mL). The product was then diluted with EtOAc (150 mL) before it was washed with water (200 mL). The aqueous phase was re-extracted with EtOAc (50 mL). The combined organic phases were then washed with water (3 × 50 mL), sat. $NaHCO_3$ (3 × 50 mL) and brine (50 mL). The product was dried ($MgSO_4$), filtered and concentrated to dryness to yield the crude *hemiacetal* **10** as a white foam (5.8 g) which was used without further purification. ^{1}H NMR analysis of the crude product confirmed the identity of **10**. R_f = 0.10 (PhMe/EtOAc 3:1;

stains brown with *p*-anisaldehyde/H_2SO_4 dip). HRMS: calcd for $C_{13}H_{18}O_{10}Na$ 357.0798 $[M + Na]^+$; found 357.0417 $[M + Na]^+$.

Methyl (2,3,4-tri-*O*-acetyl-α-D-mannopyranosyl fluoride)uronate (4α) and Methyl (2,3,4-tri-*O*-acetyl-β-D-mannopyranosyl fluoride)uronate (4β): To a stirred solution of anhydrous Et_3N (2.4 mL, 17 mmol) under $Ar_{(g)}$ at r.t. in dry CH_2Cl_2 (40 mL) was added $Et_3N{\cdot}3HF$ (5.7 mL, 35 mmol) dropwise over 2 min. The mixture was stirred for a further 5 min before XtalFluor-M® (6.32 g, 26 mmol) was added in one portion under a stream of $Ar_{(g)}$. The resulting red solution was placed in a dry ice/acetone bath (external Dewar temperature: -76°C) before a solution of the crude hemiacetal 10 (5.8 g, ~ 17 mmol) in dry CH_2Cl_2 (40 mL) was added dropwise over 8 min. Stirring was continued at the same temperature for 2 h. The reaction was quenched with sat. $NaHCO_3$ (50 mL) which was added in 10 mL portions over a 5 min period. The icy mixture was allowed to slowly attain r.t. after which stirring was continued for 30 min and the solution became colourless. The mixture was then diluted with $CHCl_3$ (150 mL) before it was washed with water (50 mL) and brine (50 mL). The product was dried ($MgSO_4$), filtered and concentrated to dryness. ^1H and ^{19}F NMR analysis of the crude product mixture revealed a 51:49 isomeric ratio of **4α**:**4β**. Purification by flash chromatography (PhMe/EtOAc 10:1 → 6:1 → 3:1) afforded 4.2 g (58%, 2 steps) of *fluorides* **4α** and **4β** as a colourless syrup. Crystals of both anomers were grown from *n*-hexane/EtOAc (colourless needles) following chromatographic enrichment to >85%. These samples were subjected to mass spectral, melting point and/or X-ray crystallographic analysis. Data for **4α**: R_f = 0.40 (PhMe/EtOAc 3:1; stains brown with *p*-anisaldehyde/H_2SO_4 dip), m.p. 94 – 96 °C. ^1H NMR (500 MHz, $CDCl_3$): δ 5.65 (dd, 1H, $J_{1,2}$ = 2.4 Hz, $J_{1,F}$ = 48.4 Hz, H-1), 5.46 – 5.37 (m, 3H, H-2, H-3, H-4), 4.44 (d, 1H, $J_{4,5}$ = 9.5 Hz, H-5), 3.78 (s, 3H, CO_2CH_3), 2.17 (s, 3H, -CH_3), 2.06 (s, 3H, -CH_3), 2.02 (s, 3H, -CH_3). ^{13}C NMR (125 MHz, $CDCl_3$): δ 169.9, 169.7, 169.5, 167.1 (4 × C=O), 104.5 (d, $J_{1,F}$ =

223.5 Hz, C-1), 70.9 (d, $J_{5,F}$ = 3.0 Hz, C-5), 67.4 (C-3), 67.2 (d, $J_{2,F}$ = 38.2 Hz, C-2), 65.9 (C-4), 53.0 (CO_2CH_3), 20.7, 20.5(3), 20.5(2) (3 × -CH_3). ^{19}F NMR (470 MHz, $CDCl_3$): δ -139.2 (ap. d, $J_{1,F}$ = 48.5 Hz). HRMS: calcd for $C_{13}H_{17}FO_9Na$ 359.0755 $[M + Na]^+$; found 359.0845 $[M + Na]^+$. Key data for **4β**: R_f 0.39 (PhMe/EtOAc 3:1; stains brown with *p*-anisaldehyde/H_2SO_4 dip), m.p. 84-86 °C. ^{1}H NMR (500 MHz, $CDCl_3$): δ 5.66 (dd, 1H, $J_{1,2}$ = 2.5 Hz, $J_{1\text{-}F}$ = 51.8 Hz, H-1), 5.64 (dd, 1H, $J_{3,4}$ = 6.4 Hz, $J_{4,5}$ = 4.3 Hz, H-4), 5.34 (ddd, 1H, $J_{2,3}$ = 3.4 Hz, $J_{2\text{-}F}$ = 17.3 Hz, H-2), 5.22 (dd, 1H, H-3), 4.38 (d, 1H, H-5), 3.81 (s, 3H, CO_2CH_3), 2.15 (s, 3H, -CH_3), 2.12 (s, 3H, -CH_3), 2.05 (s, 3H, -CH_3). ^{13}C NMR (125 MHz, $CDCl_3$): δ 169.9, 169.6, 169.2, 167.2 (4 × C=O), 103.4 (d, $J_{1,F}$ = 231.7 Hz, C-1), 72.0 (d, $J_{5,F}$ = 2.5 Hz, C-5), 67.2 (C-4), 66.5 (d, $J_{3,F}$ = 2.2 Hz, C-3), 65.3 (d, $J_{2,F}$ = 20.9 Hz, C-2), 53.0 (CO_2CH_3), 20.9, 20.8, 20.6 (3 × -CH_3). ^{19}F NMR (470 MHz, $CDCl_3$): δ -142.4 (dd, $J_{1,F}$ = 51.8 Hz, $J_{2,F}$ = 17.3 Hz). HRMS: calcd for $C_{13}H_{17}FO_9Na$ 359.0755 $[M + Na]^+$; found 359.0737 $[M + Na]^+$.

Methyl (2,3,4-tri-*O*-acetyl-5-*C*-bromo-β-D-mannopyranosyl fluoride)uronate (2): *Method 1*. A vigorously stirred suspension of the glycosyl fluorides **4α** and **4β** (13:87 **4α**:**4β**; 205 mg, 0.61 mmol), Br_2 (63 µL, 1.2 mmol) and K_2CO_3 (42 mg) in dry $PhCF_3$ (42 mL) under $Ar_{(g)}$ was irradiated at 70 °C for 3 h. The reaction was then cooled to r.t. before it was diluted with EtOAc (50 mL) and washed with sat. $Na_2S_2O_3$ (20 mL), water (20 mL) and brine (20 mL). The product was then dried ($MgSO_4$), filtered and concentrated under reduced pressure (rotary evaporator water bath temperature < 30 °C). Purification by flash chromatography (SiO_2, PhMe/EtOAc 5:1 → 2:1 → 1:1) gave the *bromide* **2** as a yellow oil (145 mg, 57%). **4α** (9 mg, 4%) was recovered. R_f = 0.66 (PhMe/EtOAc 4:1; stains green/brown with *p*-anisaldehyde/H_2SO_4 dip). ^{1}H NMR (500 MHz, $CDCl_3$): δ 5.87 (dd, 1H, $J_{1,2}$ = 1.5 Hz, $J_{1,F}$ = 47.0 Hz, H-1), 5.71 – 5.69 (m, 1H, H-2), 5.53 (d, 1H, $J_{3,4}$ = 10.0 Hz, H-4), 5.36 (ddd, 1H, $J_{2,3}$ = 3.2 Hz, $J_{3,F}$ = 1.5 Hz, H-3), 3.88 (s, 3H, CO_2CH_3), 2.19 (s, 3H, -CH_3), 2.12 (s, 3H, -CH_3), 2.02 (s, 3H, -CH_3). ^{13}C NMR

(125 MHz, $CDCl_3$): δ 169.7, 169.6, 169.0, 164.1 (4 × C=O), 103.9 (d, $J_{1,F}$ = 225.2 Hz, C-1), 88.9 (d, $J_{5,F}$ = 8.1 Hz, C-5), 68.3 (d, $J_{3,F}$ = 9.4 Hz, C-3), 66.5 (d, $J_{2,F}$ = 17.2 Hz, C-2), 66.4 (C-4), 54.2 (CO_2CH_3), 20.7, 20.6, 20.4 (3 × -CH_3). ^{19}F NMR (470 MHz, $CDCl_3$): δ -153.9 (ap. d, $J_{1,F}$ = 47.0 Hz). HRMS: calcd for $C_{13}H_{16}BrFO_9Na$ 436.9860 $[M + Na]^+$; found 436.9836 $[M + Na]^+$.

Method 2: Recrystallized **4b** (194 mg, 0.58 mmol) and NBS (310 mg, 1.74 mmol, 3.0 eq.) were dissolved with anhydrous $PhCF_3$ (0.16 M). Br_2 (2.5 mol%) was then added into the reaction mixture with a microliter syringe (5 mL). The reaction mixture was placed into the compact photoreactor and irradiated (purple LEDs, λ=405 nm, 8.7W) under Ar(g) for 1.5 h. The reactor was cooled by air flow such that the temperature was maintained ~40 °C. The reaction mixture was then diluted with EtOAc and the organic phase was washed with 50% $Na_2S_2O_3$ (×1), sat. $NaHCO_3$ (×1) and brine (×3) before it was dried ($MgSO_4$), filtered and concentrated to dryness. The residue was purified by flash chromatography (PhMe/EtOAc 20:1) to give the bromide **2** as a colourless syrup (217 mg, 91%), $[\alpha]_D$ -124.0 (*c.* 2.7, $CHCl_3$). R_f (PhMe/EtOAc, 20:1) = 0.3. The NMR spectra were identical to that prepared by method 1.

Reduction of 2 with *n*-Bu_3SnH: A stirred solution of the bromide **2** (115 mg, 0.28 mmol) in anhydrous PhMe (7 mL) under $Ar_{(g)}$ was treated successively at r.t. with Et_3B (27 µL, 1.0 M solution in hexanes, 0.03 mmol) and *n*-Bu_3SnH (300 µL, 1.0 M solution in hexanes, 0.30 mmol). The reaction was continued for 50 min before it was concentrated to dryness. The crude oily residue was taken up in acetonitrile (50 mL) and washed with *n*-hexane (3 × 15 mL). The acetonitrile phase was then concentrated under reduced pressure. ^{1}H NMR analysis of the crude product mixture revealed an 82:18 isomeric ratio of *fluorides* **3**:**4β**. Purification by flash chromatography (PhMe/EtOAc 4:1 → 2:1) furnished an inseparable mixture of **3** and **4β** as a colourless syrup (87 mg, 93%).

Reduction of 2 with $InCl_3/Et_3SiH$: $InCl_3$ (43 mg, 0.19 mmol) was heated under high vacuum at 110 °C for 1h. The flask was then back-filled with dry $Ar_{(g)}$ before dry CH_3CN (1 mL) was added. The solution was cooled in an ice-water bath (external Dewar temperature: 4 °C) and Et_3SiH (31 µL, 0.19 mmol) was added dropwise over 1 min. Stirring was continued for 10 min after which a solution of **2** (40 mg, 0.09 mmol) in dry CH_3CN (1 mL) was added dropwise over 1 min followed by Et_3B (19 µL, 1.0 M in hexanes, 0.02 mmol) in one portion. The reaction was stirred for a further 5 min before it was warmed to r.t. and stirred for 10 min. After this time, the reaction was quenched in an ice-water bath with sat. $NaHCO_3$ (1 mL) which generated a white precipitate. The product was then diluted with EtOAc (20 mL), washed with water 20 (mL) and brine (20 mL) before it was dried ($MgSO_4$), filtered and concentrated to dryness. ^1H NMR analysis of the crude product mixture revealed an 87:13 isomeric ratio of *fluorides* **3**:**4β**. Purification by flash chromatography (PhMe/EtOAc 4:1 → 2:1) furnished an inseparable mixture of **3** and **4β** as a colourless syrup (27 mg, 83%).

Photochemical resolution of methyl (2,3,4-tri-*O*-acetyl-α-L-gulopyranosyl fluoride)uronate(3): An azeotropically dried mixture of fluorides **3** and **4β** (64 mg, 0.19 mmol; 82:18 3:4β) was taken up in dry $PhCF_3$ (14 mL). Br_2 (10 µL, 0.19 mmol) and K_2CO_3 (14 mg) were added and the resulting red suspension was irradiated at 70 °C with vigorous stirring under $Ar_{(g)}$ for 1h. After this time, irradiation was ceased and the product mixture was cooled to r.t. It was then diluted with EtOAc (50 mL) and washed with sat. $Na_2S_2O_3$ (20 mL), sat. $NaHCO_3$ (20 mL) and brine (20 mL). The product was dried ($MgSO_4$), filtered and concentrated to dryness. Purification by flash chromatography (*n*-hexane/EtOAc 5:1 → 3:1→ 1:1→ 1:2) furnished 27 mg (42%) of *fluoride* **3** as a colourless oil and 17 mg (21%) of *bromide* **2**. Data for **3**: R_f = 0.32 (PhMe/EtOAc 4:1; stains brown/purple with *p*-anisaldehyde/H_2SO_4

dip). $[\alpha]_D$ -54.9 (*c*. 0.49, $CHCl_3$).^{1}H NMR (500 MHz, $CDCl_3$): δ 5.75 (dd, 1H, $J_{1,2}$ = 3.6 Hz, $J_{1,F}$ = 53.5 Hz, H-1), 5.39 (ddd, 1H, $J_{2,3}$ = 5.0 Hz, $J_{3,4}$ = 4.1 Hz, $J_{3,F}$ = 1.1 Hz, H-3), 5.36 (dd, 1H, $J_{4,5}$ = 1.8 Hz, H-4), 5.12 (ddd, 1H, $J_{2,F}$ = 26.6 Hz, H-2), 4.97 (d, 1H, H-5), 3.78 (s, 3H, CO_2CH_3), 2.17 (s, 3H, -CH_3), 2.12 (s, 3H, -CH_3), 2.08 (s, 3H, -CH_3). ^{13}C NMR (125 MHz, $CDCl_3$): δ 169.6, 169.3, 168.9, 167.1 (4 × C=O), 103.8 (d, $J_{1,F}$ = 235.6 Hz, C-1), 68.6 (C-4), 67.3 (d, $J_{5,F}$ = 3.0 Hz, C-5), 65.2 (C-3), 64.8 (d, $J_{2,F}$ = 21.2 Hz, C-2), 52.8 (CO_2CH_3), 20.7, 20.5(1), 20.5(0) (3 × C=O). ^{19}F NMR (470 MHz, $CDCl_3$): δ -148.2 (dd, $J_{1,F}$ = 52.3 Hz, $J_{2,F}$ = 26.0 Hz). HRMS: calcd for $C_{13}H_{17}FO_9Na$ 359.0755 $[M + Na]^+$; found 359.0845 $[M + Na]^+$.

Computational details: We modelled the reduction of bromide **2** using a similar approach to that which was employed in our previous studies.[12] Density functional theory calculations were performed using Gaussian 16.[30] The conformations of transition states were explored by means of a conformational search in MacroModel 10.6,[31] using the MCMM torsional sampling algorithm in conjunction with the OPLS3e forcefield[32] with a dielectric constant set to e = 2.3 to mimic that of toluene (e = 2.37). In this search, the lengths and angles of the forming and breaking bonds were fixed while the pyranose ring was left unrestricted. For each transition state, the 5 lowest energy conformations were then subjected to DFT optimisation using the B3LYP33 functional and a basis set consisting of LANL2DZ on Sn and 6-31G(d) on all other atoms. The optimizations were conducted in implicit toluene, as modelled with the SMD implicit solvent model.[14] Harmonic vibrational frequency calculations were performed to confirm that the stationary points were indeed transition states (one imaginary frequency), and also to compute zero-point energies and thermochemical corrections. Truhlar's quasiharmonic approximation was used to correct errors in computed entropies.[34] By this method, all harmonic frequencies below 100 cm^{-1} were raised to exactly 100 cm^{-1} after which the vibrational component of the thermal contribution to entropy was evaluated. Single-point energy

calculations were then performed at the B3LYP-D3(BJ)35/def2-TZVPP-SMD(toluene) level of theory. Solution-phase free energies were computed by adding the B3LYP zero-point energy and thermochemical corrections to the B3LYP-D3(BJ) solution-phase electronic energies. A standard state of 298.15 K and 1 mol L^{-1} was used.

X-ray crystallographic studies: An Oxford Diffraction Gemini CCD diffractomer was used to acquire the crystallographic data for glycosyl fluorides **4α** and **4β** operating within a range of $2 < 2\theta < 125$ Å. Cu-Kα radiation was used (1.5418 Å). Empirical absorption corrections (multi-scan) and data reduction were performed with Oxford Diffraction CrysAlisPro software (Oxford Diffraction, vers. 171.40.53). An Oxford Cryosystems Desktop Cooler was used to cool the crystals. Structures were solved with SIR92 and refined by full-matrix least-squares analysis with SHELXL.[36] All non-H atoms were refined with anisotropic thermal parameters while H-atoms were included at calculated positions using a riding model. Mercury was used to produce the graphics.[37] WinGX was used for all calculations.[38]

ASSOCIATED CONTENT

Supporting Information

Cartesian coordinates for calculated transition states, and copies of ^{1}H, ^{13}C and ^{19}F NMR spectra (PDF).

The Supporting Information is available free of charge on the ACS Publications website.

AUTHOR INFORMATION

Corresponding Author

*Vito Ferro – School of Chemistry and Molecular Biosciences, The University of Queensland, Brisbane QLD 4072, Australia. Email: v.ferro@uq.edu.au

Author Contributions

The manuscript was written through contributions of all authors. All authors have given approval to the final version of the manuscript.

Notes

The authors declare no competing financial interest.

ACKNOWLEDGMENTS

We thank the Australian Research Council for financial support (DP220102493). NWS is grateful to the University of Queensland (UQ) for a PhD scholarship. We thank Prof. Paul Bernhardt (UQ) for collecting the X-ray diffraction data and we acknowledge Mr Jacob Cameron and Ms Charne Crous for technical assistance. Computational resources were provided by the University of Queensland Research Computing Centre.

REFERENCES

1. (a) Ahmad, A.; Mubarak, N. M.; Jannat, F. T.; Ashfaq, T.; Santulli, C.; Rizwan, M.; Najda, A.; Bin-Jumah, M.; Abdel-Daim, M. M.; Hussain, S., et al., A critical review on the synthesis of natural sodium alginate based composite materials: an innovative biological polymer for biomedical delivery applications. *Processes* **2021,** *9*, 137; (b) Cao, Y.; Cong, H.; Yu, B.; Shen, Y., A review on the synthesis and development of alginate hydrogels for wound therapy. *J. Mater. Chem. B* **2023,** *11*, 2801-2829; (c) Lee, K. Y.; Mooney, D. J., Alginate: properties and biomedical applications. *Prog. Polym. Sci.* **2012,** *37*, 106-126; (d) Li, J.; Cai, C.; Yang, C.; Li, J.; Sun, T.; Yu, G., Recent advances in pharmaceutical potential of brown algal polysaccharides and their derivatives. *Curr. Pharm. Des.* **2019,** *25*, 1290-1311; (e) Pawar, S. N.; Edgar, K. J.,

Alginate derivatization: a review of chemistry, properties and applications. *Biomaterials* **2012,** *33*, 3279-3305.

2. Cryz, S. J.; Furer, E.; Que, J. U., Synthesis and characterisation of a *Pseudomonas aeuroginosa* alginate-toxin-A conjugate vaccine. *Infect. Immun.* **1991,** *59*, 45-50.
3. van den Bos, L. J.; Dinkelaar, J.; Overkleeft, H. S.; van der Marel, G. A., Stereocontrolled synthesis of β-D-mannuronic acid esters: synthesis of an alginate trisaccharide. *J. Am. Chem. Soc.* **2006,** *128*, 13066-13067.
4. Dinkelaar, J.; van den Bos, L. J.; Hogendorf, W. F. J.; Lodder, G.; Overkleeft, H. S.; Codée, J. D. C.; van der Marel, G. A., Stereoselective synthesis of L-guluronic acid alginates. *Chem. Eur. J.* **2008,** *14*, 9400-9411.
5. Zhang, Q.; van Rijssel, E. R.; Walvoort, M. T.; Overkleeft, H. S.; van der Marel, G. A.; Codée, J. D., Acceptor reactivity in the total synthesis of alginate fragments containing α-L-guluronic acid and β-D-mannuronic acid. *Angew. Chem. Int. Ed.* **2015,** *54*, 7670-3.
6. Kinnaert, C.; Daugaard, M.; Nami, F.; Clausen, M. H., Chemical synthesis of oligosaccharides related to the cell walls of plants and algae. *Chem. Rev.* **2017,** *117*, 11337-11405.
7. Li, X.; Wang, D.; Zhang, P.; Yu, G.; Cai, C., Recent advances in the chemical synthesis of marine acidic carbohydrates. *Curr. Org. Chem.* **2021,** *25*, 507-518.
8. Li, S.; Wang, Z.; van der Marel, G. A.; Codée, J. D. C., Synthesis of uronic acid containing oligosaccharides. In *Comprehensive Glycoscience* 2nd ed.; Barchi, J. J., Ed. Elsevier: Oxford, 2021; pp 200-227.
9. Zhang, L.; Zhang, Y.; Hua, Q.; Xu, T.; Liu, J.; Zhu, Y.; Yang, Y., Promoter-controlled synthesis and antigenic evaluation of mannuronic acid alginate glycans of *Pseudomonas aeruginosa*. *Org. Lett.* **2022,** *24*, 8381-8386.

10. Biosynth Catalogue. Prices are based on the 50 mg (D-ManA), 25 mg (L-GulA) and 10,000 mg (L-gulose) packs which are the maximum sizes available. https://www.biosynth.com/ Accessed: May, 2023.

11. van den Bos, L. J.; Codée, J. D. C.; van der Toorn, J. C.; Boltje, T. J.; van Boom, J. H.; Overkleeft, H. S.; van der Marel, G. A., Thioglycuronides: synthesis and application in the assembly of acidic oligosaccharides. *Org. Lett.* **2004,** *6*, 2165-2168.

12. (a) Mohamed, S.; Krenske, E. H.; Ferro, V., The stereoselectivities of tributyltin hydride-mediated reductions of 5-bromo-D-glucuronides to L-iduronides are dependent on the anomeric substituent: syntheses and DFT calculations. *Org. Biomol. Chem.* **2016,** *14*, 2950-2960; (b) See, N. W.; Wimmer, N.; Krenske, E. H.; Ferro, V., A substituent-directed strategy for the selective synthesis of L-hexoses: an expeditious route to L-idose. *Eur. J. Org. Chem.* **2021,** *2021*, 1575-1584.

13. Herczeg, M.; Demeter, F.; Lisztes, E.; Racskó, M.; Tóth, B. I.; Timári, I.; Bereczky, Z.; Kövér, K. E.; Borbás, A., Synthesis of a heparinoid pentasaccharide containing L-guluronic acid instead of L-iduronic acid with preserved anticoagulant activity. *J. Org. Chem.* **2022,** *87*, 15830-15836.

14. See, N. W.; Wimmer, N.; Pierens, G. K.; Krenske, E. H.; Ferro, V., C-5 Epimerisation of D-mannopyranosyl fluorides: the influence of anomeric configuration on radical reactivity. *Synthesis* **2023**, DOI: 10.1055/a-2149-4586.

15. Marenich, A. V.; Cramer, C. J.; Truhlar, D. G., Universal solvation model based on solute electron density and on a continuum model of the solvent defined by the bulk dielectric constant and atomic surface tensions. *J. Phys. Chem. B* **2009,** *113*, 6378-6396.

16. Guindon, Y.; Slassi, A.; Rancourt, J.; Bantle, G.; Bencheqroun, M.; Murtagh, L.; Ghiro, E.; Jung, G., Role of σ-donation in the stereocontrol of hydrogen-transfer reactions involving acyclic radicals. *J. Org. Chem.* **1995,** *60*, 288-289.

17. Nicolaou, K. C.; Dolle, R. E.; Papahatjis, D. P., Practical synthesis of oligosaccharides. partial synthesis of avermectin B1a. *J. Am. Chem. Soc.* **1984,** *106*, 4189-4192.

18. See, N. W.; Xu, X.; Ferro, V., An improved protocol for the stereoselective synthesis of β-D-glycosyl fluorides from 2-*O*-acyl thioglycosides. *J. Org. Chem.* **2022,** *87*, 14230-14240.

19. L'Heureux, A.; Beaulieu, F.; Bennett, C.; Bill, D. R.; Clayton, S.; LaFlamme, F.; Mirmehrabi, M.; Tadayon, S.; Tovell, D.; Couturier, M., Aminodifluorosulfinium salts: selective fluorination reagents with enhanced thermal stability and ease of handling. *J. Org. Chem.* **2010,** *75*, 3401-3411.

20. Cleavage of the *O*-acetyl esters of **4α** and **4β** under Zémplen conditions (NaOMe/MeOH) yielded readily separable triols. However, E1cB elimination across the C-4 - C-5 bond competed strongly with the transesterification processes. .

21. Deposition numbers 2288688 (for **4α**) and 2288689 (for **4β**) contain the supplementary crystallographic data for this paper. These data are provided free of charge by the joint Cambridge Crystallographic Data Centre and Fachinformationszentrum Karlsruhe Access Structures service.

22. (a) Somsák, L.; Czifrák, K., Radical-mediated brominations at ring-positions of carbohydrates - 35 years later. *Carbohydr. Chem.* **2013,** *39*, 1-37; (b) Somsák, L.; Ferrier, R. J., Radical-mediated brominations at ring positions of carbohydrates. *Adv. Carbohydr. Chem. Biochem.* **1991,** *49*, 37-92.

23. 9 mg (4%) of **4α** was recovered from the product mixture.

24. Terstiege, I.; Maleczka, R. E., A new approach for the generation and reaction of organotin hydrides: the development of reactions catalytic in tin. *J. Org. Chem.* **1999,** *64*, 342-343.

25. Cole, S. J.; Kirwan, J. N.; Roberts, B. P.; Willis, C. R., Radical chain reduction of alkyl halides, dialkyl sulphides and *O*-alkyl *S*-methyl dithiocarbonates to alkanes by trialkylsilanes. *J. Chem. Soc. Perkin Trans. 1* **1991**, 103-112.

26. Chatgilialoglu, C.; Ferreri, C.; Landais, Y.; Timokhin, V. I., Thirty years of $(TMS)_3SiH$: a milestone in radical-based synthetic chemistry. *Chem. Rev.* **2018,** *118*, 6516-6572.

27. Unpublished results.

28. Hayashi, N.; Shibata, I.; Baba, A., Triethylsilane−indium(III) chloride system as a radical reagent. *Org. Lett.* **2004,** *6*, 4981-4983.

29. Sati, G. C.; Martin, J. L.; Xu, Y.; Malakar, T.; Zimmerman, P. M.; Montgomery, J., Fluoride migration catalysis enables simple, stereoselective, and iterative glycosylation. *J. Am. Chem. Soc.* **2020,** *142*, 7235-7242.

30. Frisch, M. J.; Trucks, G. W.; Schlegel, H. B.; Scuseria, G. E.; Robb, M. A.; Cheeseman, J. R.; Scalmani, G.; Barone, V.; Petersson, G. A.; Nakatsuji, H., et al. *Gaussian 16 Rev. C.01*, Wallingford, CT, 2016.

31. Schrödinger *MacroModel*, LLC: New York, NY, 2020.

32. Roos, K.; Wu, C.; Damm, W.; Reboul, M.; Stevenson, J. M.; Lu, C.; Dahlgren, M. K.; Mondal, S.; Chen, W.; Wang, L., et al., OPLS3e: extending force field coverage for drug-like small molecules. *J. Chem. Theory Comput.* **2019,** *15*, 1863-1874.

33. (a) Lee, C.; Yang, W.; Parr, R. G., Development of the Colle-Salvetti correlation-energy formula into a functional of the electron density. *Phys. Rev. B* **1988,** *37*, 785-789; (b) Becke, A. D., A new mixing of Hartree–Fock and local density-functional theories. *J. Chem. Phys.* **1993,** *98*, 1372-1377; (c) Becke, A. D., Density-functional thermochemistry. III. The role of exact exchange. *J. Chem. Phys.* **1993,** *98*, 5648-5652; (d) Stephens, P. J.; Devlin, F. J.; Chabalowski, C. F.; Frisch, M. J., *Ab initio* calculation

of vibrational absorption and circular dichroism spectra using density functional force fields. *J. Phys. Chem.* **1994,** *98*, 11623-11627.

34. Zhao, Y.; Truhlar, D. G., Computational characterization and modelling of buckyball tweezers: density functional study of concave-convex π-π interactions. *Phys. Chem. Chem. Phys.* **2008,** *10*, 2813-2818.

35. (a) Grimme, S.; Antony, J.; Ehrlich, S.; Krieg, H., A consistent and accurate *ab initio* parameterization of density functional dispersion correction (DFT-D) for the 94 elements H-Pu. *J. Chem. Phys.* **2010,** *132*, 154104; (b) Grimme, S.; Ehrlich, S.; Goerigk, L., Effect of the damping function in dispersion corrected density functional theory. *J. Comp. Chem.* **2011,** *32*, 1456-1465.

36. Sheldrick, G. M., A short history of SHELX. *Acta Crystallogr., Sect. A: Found. Adv.* **2008,** *64*, 112-122.

37. Macrae, C. F.; Sovago, I.; Cottrell, S. J.; Galek, P. T. A.; McCabe, P.; Pidcock, E.; Platings, M.; Shields, G. P.; Stevens, J. S.; Towler, M., et al., Mercury 4.0: from visualization to analysis, design and prediction. *J. Appl. Crystallogr.* **2020,** *53*, 226-235.

38. Farrugia, L. J., WinGX and ORTEP for Windows: an update. *J. Appl. Crystallogr.* **2012,** *45*, 849-854.

TOC GRAPHIC